Angle resolved spectroscopy of polariton stimulation under non-resonant excitation in CdTe II–VI microcavity

2004 J. Phys.: Condens. Matter 16 S3683

(http://iopscience.iop.org/0953-8984/16/35/009)

INSTITUTE OF PHYSICS PUBLISHING JOURNAL OF PHYSICS: CONDENSED MATTER

J. Phys.: Condens. Matter **16** (2004) S3683–S3688 PII: S0953-8984(04)83280-6

Angle resolved spectroscopy of polariton stimulation under non-resonant excitation in CdTe II–VI microcavity

Maxime Richard, Jacek Kasprzak, Régis André, Le Si Dang and Robert Romestain

CEA-CNRS-UJF Group 'Nanophysique et Semiconducteurs', Laboratoire de Spectrométrie Physique, Université J Fourier, Grenoble, BP87, 38402 St Martin d'Hères, France

Received 6 July 2004
Published 20 August 2004
Online at stacks.iop.org/JPhysCM/16/S3683
doi:10.1088/0953-8984/16/35/009

Abstract

We present some experimental study of CdTe II–VI microcavity polaritons generated by strong non-resonant optical excitation. We first compare spectra of luminescence under high excitation and white light reflectivity showing that the polariton stimulation occurs in the strong coupling regime. In a second part we present a measurement of the integrated polariton emission intensity versus the excitation power: the stimulated emission exhibits an exponential behaviour which excludes a polariton/polariton quadratic collision process. In a third part we present an angle-resolved experiment showing that the stimulation peak is dispersion free while the residual spontaneous emission keeps its usual dispersion curve; we exclude a simple scattering phenomenon due to surface roughness and discuss the possibility of real space shrinkage or polariton collisions within a coherent population inspired by the theoretical work of Ciuti and co-workers.

1. Introduction

The exciton polariton is the lowest energy mode of semiconductor microcavities under the strong coupling regime, and consists of a coherent mixing of a quantum well exciton and a cavity photon. This composite nature gives the polariton two main features: the exciton part allows relaxation processes crucial for population redistribution; the photonic part is responsible for a very steep dispersion curve that can act as a polariton trap that contains very few states (typically around 300 for a 50 μm^2 quantization area). The polariton is therefore very suitable for a single-state high filling effect; it is actually considered as the best candidate for achievement of Bose–Einstein condensation in solids (BEC) [3]. Some very significant observations of stimulation have been obtained already in both III–V [5] and II–VI [4] microcavities under resonant and non-resonant excitation respectively. In this work we

focus on this stimulation effect in II–VI microcavities under strong non-resonant excitation: in the first part we present evidence for strong coupling in the stimulation regime. In the second part we show that the emission intensity dependence on excitation power is definitely faster than quadratic. In the third part we present a measurement of the stimulation peak dispersion by an angle resolved experiment.

2. Experimental setup

Our setup allows one to probe the lower polariton (LP) branch states by angle resolved spectroscopy experiments: the sample consists of a 16 QW microcavity with a vacuum Rabi splitting of 26 meV. It is mounted in a high numerical aperture cryostat where it is cooled down to 5 K by thermal conduction. It is optically excited by 500 fs titanium–sapphire pulses focused on a 10 μm spot radius on the sample; the energy of the laser is tuned to excite electron–hole pairs in the QWs at 100 meV above the uncoupled exciton energy. The carriers created by this means relax quickly ($<$1 ps) into hot excitons by LO phonon emission and then into polariton states after several slower relaxation processes where the laser coherence has no chance to be conserved. The polariton luminescence is then collected through a multimode fibre that can rotate away from the sample growth axis, and injected into a monochromator. The angular resolution achieved in this set-up is 1°. The in-plane wavevector is connected to the external angle θ_{ext} of collection by the simple relation

$$k_{\parallel} = \frac{E_{\mathrm{LP}}(\theta_{\mathrm{ext}})}{\hbar c} \sin(\theta_{\mathrm{ext}}). \tag{1}$$

Thus the angle resolved experiment allows one to probe the polariton states individually. It is also possible to measure the reflectivity of the same point on the sample with the use of a tungsten white light and a microscope objective; the reflectivity spectra obtained are integrated over $\pm 10°$.

Figure 1 displays the typical luminescence spectrum obtained at 0° collection angle under strong excitation (lower spectrum): an intense and narrow line appears on the high energy side of the spontaneous broad emission line. Its intensity exhibits an exponential increase with the excitation power as will be discussed in the next section. It has already been shown that this laser-like behaviour cannot be explained in terms of population inversion of an electron–hole plasma [4]: the strong coupling in this regime would be destroyed and the lasing peak would appear at the energy of the uncoupled cavity mode. Yet figure 1 shows that the stimulated narrow peak appears 7.8 meV below the uncoupled cavity mode and is blue shifted by 2 meV with respect to the lower polariton mode. Moreover, we estimate the exciton density to be 5×10^{10} cm^{-2} at threshold. This value is about one order of magnitude smaller than the exciton screening density n_{s} which is connected to the effective Bohr radius a_{B}^{*} [2] (3.6 nm for a 8 nm thick CdTe QW):

$$n_{\mathrm{s}} = \frac{1}{8.51\pi a_{\mathrm{B}}^{*2}} = 3 \times 10^{11}\ \mathrm{cm}^{-2}. \tag{2}$$

The strong coupling is thus definitely conserved in this excitation regime and the process creating this stimulated peak involves polaritonic states.

3. Non-linear emission

Setting the detection angle at 0° (detuning is $\delta = -10$ meV) we recorded polariton luminescence spectra versus the excitation power; the spectra are then integrated over the

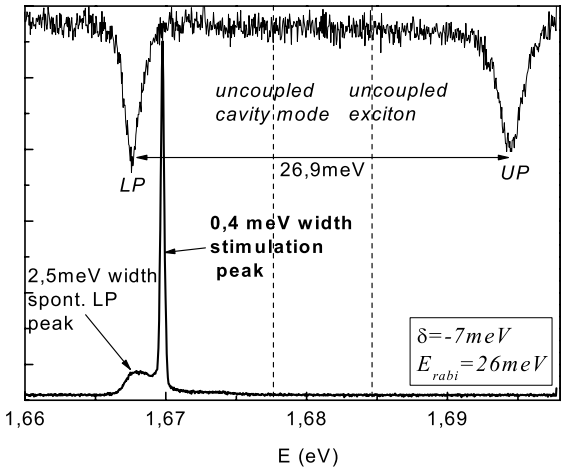

Figure 1. Upper line: reflectivity at point P on the sample corresponding to the detuning $\delta = -7$ meV; the low energy dip is the lower polariton mode (LP); the high energy one is the upper polariton mode (UP). Lower line: time integrated emission spectrum under strong excitation of the same point P: the broad (2.5 meV) small peak is a residue of spontaneous polariton emission; on its high energy wing is the narrow (0.4 meV width) and intense stimulation peak. The dashed lines display the energy of the uncoupled exciton and photon modes.

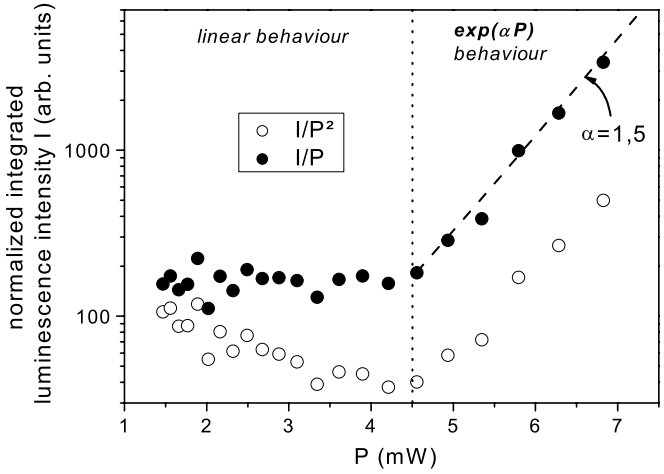

Figure 2. Dependence on the excitation power of the integrated intensity of the polariton luminescence, normalized to the excitation power (solid symbol), and normalized to the square of the excitation power (open symbol).

polariton spectrum and plotted versus excitation power. A typical result is presented in figure 2: the luminescence intensity normalized to the pump power (solid symbol) is plotted versus excitation power; for the lowest powers, the plot is constant as expected for a linear dependence on excitation power, and above a threshold (4.5 mW) it exhibits a super-linear behaviour. A quadratic behaviour would be expected in a simple process of polariton–polariton collision without any stimulation process involving the bosonic nature of the polariton; so we plot the luminescence intensity normalized to the square of the excitation power versus the excitation power (open symbol), so that a quadratic behaviour would appear constant. The figure shows

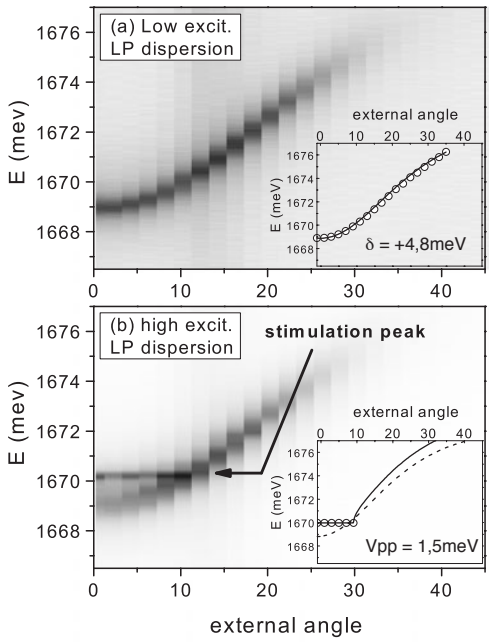

Figure 3. 3D images of polariton luminescence: vertical and horizontal axes correspond to the energy and collection angles, respectively. Polariton luminescence intensity is on a linear grey scale: the darker the grey level, the brighter the luminescence intensity. Each image is rebuilt from several spectra taken at different angles. The top image (a) was obtained for low power excitation; the polariton peak follows its usual dispersion curve. The inset displays the peak maxima of the images (circle symbol) and the corresponding calculation based on a transfer matrix method (solid curve). The bottom image (b) was obtained under strong excitation power $P = 1.05P_{\mathrm{th}}$ where P_{th} is the stimulation threshold power. The inset displays the peak maxima of the stimulation peak (circle symbol) and the calculation of the dispersion of polaritons of the states $k_{\|} = 0$ in the condensed phase (solid curve).

that, above threshold, this plot still grows by one order of magnitude within the small range considered. The emission intensity above threshold is thus over quadratic: in fact, we can fit it with an $\exp(\alpha P)$ law ($\alpha = 1.5$) which is consistent with a stimulation process.

4. Dispersion of the stimulated peak

In this section we present an angle-resolved spectroscopy of polariton emission under strong excitation at +4.8 meV detuning: the result is displayed in figure 3. Each image is built from several spectra taken at different angles: the vertical axis is the energy in meV, the horizontal axis is the collection angle, and the grey level corresponds to the intensity of the light (the darker the grey, the brighter the luminescence) at the corresponding energy. The first image (a) shows the measured polariton luminescence dispersion under weak excitation. The inset displays the corresponding luminescence peak (round symbol) and the dispersion fitted by a transfer matrix calculation [1] with the detuning $\delta = E_X(k_{\|} = 0) - E_\gamma(k_{\|} = 0)$ as the only adjustable parameter. The second image (b) shows the results obtained for an excitation power slightly above the stimulation threshold: the narrow stimulation peak appears to be dispersion free. This observation can have several explanations: scattering, shrinkage of the emitter area (diffraction) and coherent polariton/polariton collision.

4.1. Scattering by defects

The scattering by a rough surface hypothesis does not hold because the spontaneous and stimulation peaks would both be affected, yet the polariton spontaneous peak keeps its usual dispersion over the range (0°–10°) while the stimulation peak dispersion is flat. Moreover, one would expect the scattered light angular pattern to be symmetric with respect to its intensity maximum, yet the intensity of the stimulated peak is maximum when resonant with the spontaneous LP branch (at 10°) and null for larger angles.

4.2. Diffraction

The diffraction induced by a small size emitter could also explain the dispersion free emission line. The measured angular extent $\Delta\theta = 10°$ would indeed be achieved if the emitter diameter d were

$$d = 0.61\frac{2\lambda}{\Delta\theta} \sim 5\ \mu\text{m} \tag{3}$$

where $\lambda = 740$ nm is the wavelength of the peak. Some preliminary spatial imaging experiments show indeed that the size of the area responsible for the stimulation peak emission is much smaller than the 20 μm excitation spot. But the question has still to be seriously investigated and remains open.

4.3. Coherent collision of polaritons

An alternative hypothesis relies on the possibility of coherent collision within a coherent condensate of polaritons (see Ciuti *et al* [6, 7]): this model was developed for the parametric oscillation phenomenon in microcavities where a polaritonic state is given a high occupancy factor (namely, occupied by more than one in-phase polariton), by resonant pumping (pump state); two other states (signal and idler states, defined by the in-plane wavevector and energy conservations) are then also likely to get a high occupancy factor by coherent collision (without phase loss in the process) of two polaritons in the pump state. Our situation is very similar: although we do not excite resonantly, a high occupancy factor (in a state k_C around $k_\parallel = 0$) seems to be spontaneously achieved. This theory predicts that some coherent collision of two polaritons in this state would give rise to a flattening of its dispersion curve whose extent in k-space depends on the strength of the interaction between them. The inset of image (b) shows the application of such a model to our measurement (solid curve), and the value of the polariton/polariton interaction energy $V_{PP} = 1.5$ meV deduced from the extent of the stimulation peak in k-space. This value is to be compared with the analytical expression of V_{PP} [6]:

$$V_{PP} = \frac{6e^2 a_B^*}{\epsilon A} X_{k_C}^8 \langle N_P \rangle \tag{4}$$

where ϵ is the dielectric constant in F m^{-1}, A the quantization area that we assume to be the spot area (10 μm radius), X_{k_C} the Hoppfield coefficient of the state k_C, and $\langle N_P \rangle$ the average number of polaritons of the state k_C where condensation takes place. In order to adjust the analytical value to the experimental one, we have to consider an average number of condensed polaritons $\langle N_P \rangle = 10^5$.

This value is huge: one could indeed expect a smaller one for an excitation regime so close to the threshold; moreover, according to this model, the extent in angles of the stimulation peak should increase with the number of condensed polaritons, namely, with the excitation power; yet we have not observed such a behaviour.

5. Conclusion

It is thus established that the non-linear emission of microcavities takes place in the strong coupling regime, and involves polaritonic states. We show that the emission in this regime exhibits a flat dispersion curve; two hypotheses remain open to explain this feature: a shrinkage of the emitting area when entering the non-linear regime on the one hand, and a coherent polariton/polariton collision process on the other. In the near future, this last model will be compared with a direct measurement of the average number of polaritons above threshold using the intensity of the emitted beam. A spectrally resolved micro-photoluminescence set-up is also under development in order to observe some real space shrinkage of the emitting area.

Acknowledgments

We acknowledge the support of the European community for research training networks, contract number HPRN-CT-2002-00298, 'Photon-mediated phenomena in semiconductor nanostructures'. The PhD student JK gratefully acknowledges the financial support provided from the above project.

References

[1] Savona V 1999 *Confined Photon Systems: Fundamentals and Applications* (Berlin: Springer)
[2] Schmitt-Rink S, Chemla D S and Miller D A B 1985 *Phys. Rev.* B **32** 6601
[3] Porras D, Ciuti C, Baumberg J J and Tejedor C 2002 *Phys. Rev.* B **66** 085304
[4] Dang L S, Heger D, André R, Boeuf F and Romestain R 1998 *Phys. Rev. Lett.* **81** 3920
[5] Savvidis P G, Baumberg J J, Stevenson R M, Skolnick M S, Whittaker D M and Roberts J S 2000 *Phys. Rev. Lett.* **84** 1547
[6] Ciuti C, Schwendimann P, Deveaud B and Quattropani A 2000 *Phys. Rev.* B **62** R4825
[7] Ciuti C, Schwendimann P and Quattropani A 2001 *Phys. Rev.* B **63** 41303